doi:10.1111/evo.12457

GENOMIC AND MORPHOLOGICAL ANALYSIS OF A SEMIPERMEABLE AVIAN HYBRID ZONE SUGGESTS ASYMMETRICAL INTROGRESSION OF A SEXUAL SIGNAL

Daniel T. Baldassarre,[1,2,3] Thomas A. White,[4] Jordan Karubian,[5] and Michael S. Webster[1,2]

[1]*Department of Neurobiology and Behavior, Cornell University, Ithaca, New York 14850*

[2]*Macaulay Library, Cornell Lab of Ornithology, Ithaca, New York 14853*

[3]*E-mail: db547@cornell.edu*

[4]*Department of Ecology and Evolutionary Biology, Cornell University, Ithaca, New York 14850*

[5]*Department of Ecology and Evolutionary Biology, Tulane University, New Orleans, Louisiana 70118*

Received January 31, 2014
Accepted May 22, 2014

Hybrid zones are geographic regions where differentiated taxa meet and potentially exchange genes. Increasingly, genomic analyses have demonstrated that many hybrid zones are semipermeable boundaries across which introgression is highly variable. In some cases, certain alleles penetrate across the hybrid zone in only one direction, recombining into the alternate genome. We investigated this phenomenon using genomic (genotyping-by-sequencing) and morphological (plumage reflectance spectrophotometry) analyses of the hybrid zone between two subspecies of the red-backed fairy-wren (*Malurus melanocephalus*) that differ conspicuously in a sexual signal, male back plumage color. Geographic cline analyses revealed a highly variable pattern of differential introgression, with many narrow coincident clines combined with several significantly wider clines, suggesting that the hybrid zone is a semipermeable tension zone. The plumage cline was shifted significantly into the genomic background of the orange subspecies, consistent with sexual selection driving asymmetrical introgression of red plumage alleles across the hybrid zone. This interpretation is supported by previous experimental work demonstrating an extra-pair mating advantage for red males, but the role of genetic dominance in driving this pattern remains unclear. This study highlights the potential for sexual selection to erode taxonomic boundaries and promote gene flow, particularly at an intermediate stage of divergence.

KEY WORDS: **Genotyping-by-sequencing, geographic clines, neutral diffusion, red-backed fairy-wren, reflectance spectrophotometry, tension zone.**

Hybrid zones are geographic regions where two genetically differentiated taxa distinguished by at least one heritable trait meet and interbreed, thereby potentially exchanging genes (Harrison 1990). Theory suggests that many hybrid zones are semipermeable boundaries between genomes, such that alleles at some genes introgress freely, whereas others do not. The extent of introgression depends on effects on fitness and reproductive isolation, as well as on genetic linkage relationships (Barton 1979b; Harrison 1986, 1990; Wu 2001; Morjan and Rieseberg 2004; Payseur 2010; Gompert et al. 2013). This idea has recently gained empirical support with the advent of genomic tools (Nosil et al. 2007; Fitzpatrick et al. 2009; Gompert et al. 2010; Parchman et al. 2013; Larson et al. 2014). In these cases, genes that contribute to local adaptation or reproductive isolation can cause regions of the genome to remain differentiated even in the face of ongoing gene flow at other loci. Alternatively, if the cost of hybridization is low, gene flow at certain loci may be relatively unrestricted and even beneficial (i.e., adaptive introgression, Anderson and Stebbins 1954; Arnold 2004; Hedrick 2013). Semipermeability may be particularly likely in hybrid zones

EVOLUTION
INTERNATIONAL JOURNAL OF ORGANIC EVOLUTION

between taxa at an intermediate stage of divergence where some barriers to gene flow have evolved, but reproductive isolation is incomplete. Asymmetrical introgression is a special case of differential gene flow in which alleles flow in only one direction.

Many cases of asymmetrical introgression of neutral markers have been documented (reviewed in Harrison 1990), but asymmetrical introgression of alleles underlying adaptive traits appears to be much less common (but see Parsons et al. 1993; Brumfield et al. 2001; Dasmahapatra et al. 2012; Pardo-Diaz et al. 2012). This distinction can be difficult to make when only genetic markers are considered, but analyzing phenotypic traits concurrently can strengthen our understanding of how selection affects patterns of introgression. Mathematical models suggest that strong positive selection in the alternate genomic background and/or environment is necessary for asymmetrical introgression to occur (Barton 1979b, 2001; Hedrick 2013). Several cases of asymmetrical introgression involve secondary sexual characteristics and appear to be driven by asymmetrical mating preferences (e.g., Stein and Uy 2006; Garner and Neff 2013), which are predicted to be most prevalent when taxa are at an intermediate stage of divergence (Arnold et al. 1996). In birds, recent theory suggests that extra-pair mating may be a potent mechanism promoting hybridization and introgression if females prefer heterospecific males as extra-pair mates (Hartman et al. 2011). Thus, there is mounting evidence that sexual selection, particularly among sexually promiscuous species, can erode species boundaries and promote introgression. This is in stark contrast to the large body of theory (Lande 1981; West-Eberhard 1983; Uyeda et al. 2009) and empirical research (reviewed in Panhuis et al. 2001; Ritchie 2007) on the capacity for sexual selection to promote population divergence and speciation.

The red-backed fairy-wren (*Malurus melanocephalus*), a small insectivorous passerine bird endemic to Australia, appears to exhibit asymmetrical introgression of a sexual trait. This species is highly sexually dichromatic (Schodde 1982; Rowley and Russell 1997), exhibits very high rates of extra-pair paternity (Karubian 2002; Webster et al. 2008; Varian-Ramos and Webster 2012; Varian-Ramos et al. 2012; Baldassarre and Webster 2013), and has large testes relative to body size (Rowe and Pruett-Jones 2011, 2013), all of which suggest strong sexual selection on males. Moreover, two distinct subspecies are recognized based on variation in a sexual signal, male nuptial plumage color: the western, red-backed *M. m. cruentatus* and the eastern, orange-backed *M. m. melanocephalus* (Schodde 1982; Rowley and Russell 1997; Fig. 1). Across populations, there is considerable variation in other nonsexual traits, but variation in these traits is spatially complex, and is not broadly diagnostic of the two subspecies (Baldassarre et al. 2013). The two subspecies are moderately genetically differentiated across the Carpentarian Barrier (Lee and Edwards 2008), a prominent zoogeographic barrier in northwestern Queensland that likely forced subspecies into allopatric coastal refugia during the Pleistocene (Cracraft 1986; Chivas et al. 2001; Bowman et al. 2010; Cook et al. 2012). Secondary contact between the subspecies presumably occurred once the climate ameliorated (Lee and Edwards 2008). A contact zone also exists between plumage types, but is located east of the Carpentarian Barrier and does not appear to be coincident with the location of secondary contact (Baldassarre et al. 2013; Fig. 1). Previously, we suggested that this lack of coincidence was due to asymmetrical introgression of alleles for red back plumage color across the hybrid zone, likely facilitated by sexual selection via extra-pair mating (Baldassarre et al. 2013; Baldassarre and Webster 2013).

Despite these multiple lines of evidence, a thorough genetic and morphological analysis of the hybrid zone is required to rigorously test the hypothesis that red plumage color has introgressed asymmetrically. Geographic cline theory provides a suitable framework for testing these types of hypotheses by analyzing changes in allele frequencies and quantitative traits as a function of geographic distance along a transect through a hybrid zone (Barton and Hewitt 1985; Szymura and Barton 1986). Genes and traits that are subject to similar selective pressures are predicted to have similar cline centers and widths, whereas those subject to positive selection on one side of the hybrid zone will have cline centers that are displaced from the majority of other clines (Barton 1983; Barton and Hewitt 1985). Using the reduced representation genomic approach genotyping-by-sequencing (GBS), we developed a large, genome-wide, single-nucleotide polymorphism (SNP) dataset. We then compared variation in plumage color with clinal patterns for these SNPs across a 3052 km transect through the hybrid zone. The major goals of our analyses were to employ dense geographic sampling and high-resolution genomic data to test the hypotheses that (1) the hybrid zone as determined by genetic markers is centered at the Carpentarian Barrier (sensu Lee and Edwards 2008), and (2) alleles for red plumage color have introgressed asymmetrically from *cruentatus* into the genomic background of the orange *melanocephalus* subspecies. We predicted that the majority of genetic clines would have centers located near the Carpentarian Barrier, whereas the plumage color cline would have a center shifted significantly into the background of the orange subspecies. Although we did not make any a priori predictions about patterns of genetic introgression among SNP loci, we used geographic cline theory to explore the extent of locus-specific introgression and make inferences about the strength of selection in the hybrid zone. We also considered the possibility that nonselective mechanisms (e.g., dominance, epigenetic effects) may explain the apparent lack of coincidence between the hybrid zone and the plumage contact zone.

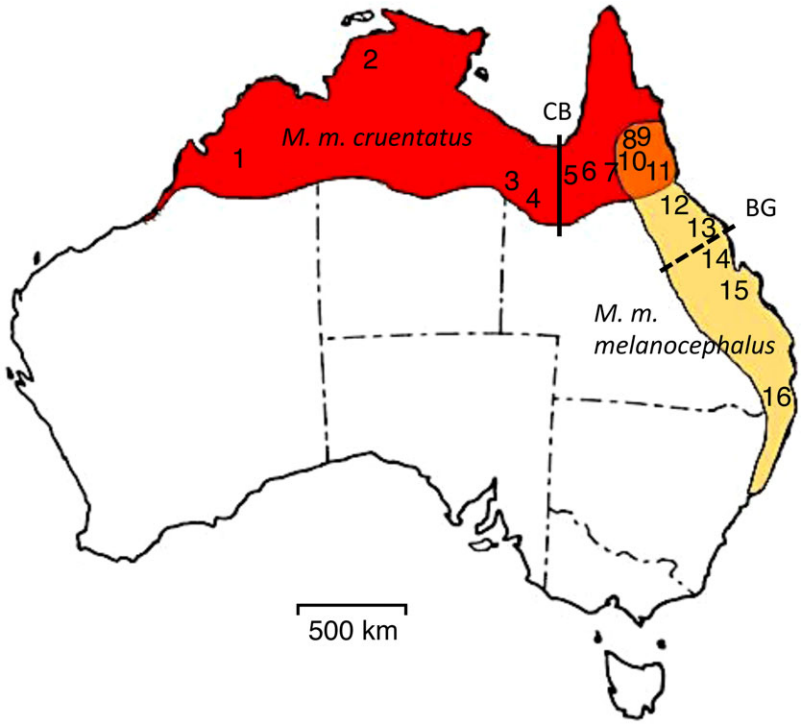

Figure 1. The species range of the red-backed fairy-wren showing the currently recognized distribution of the red *cruentatus* subspecies in the west and the orange *melanocephalus* subspecies in the east. The intermediately colored area in the northeast represents the hypothesized region of plumage overlap based on subjective evaluation of plumage color in the field. The solid line represents the Carpentarian Barrier (CB) and the dashed line represents the Burdekin Gap (BG). Numbers refer to sampling locations along the transect.

Methods

FIELD METHODS AND SAMPLING TRANSECT

From 2004 through 2011, we collected blood samples for genetic analyses and feather samples for plumage color analyses at sampling locations across the range of the red-backed fairy-wren (Fig. 1). The genetic dataset consisted of 169 individuals from 13 sampling locations, and the plumage color dataset consisted of 178 individuals from 15 sampling locations (Table 1). Birds were captured using mist nets and a small (about 50 μl) blood sample was collected and immediately stored in lysis buffer for subsequent DNA extraction. Feather samples were collected by removing a small number (about 6–12) of feathers from the center back of every captured male in nuptial plumage. We chose to collect feather samples instead of voucher specimens due to permitting restrictions and because long-term behavioral studies were being conducted at many of the sampling locations. For geographic cline analyses, we arranged sampling locations along a transect beginning with the westernmost location (Mornington), and ending at the location in the far southeast of the range (Brisbane). Each sampling location was assigned a distance along the transect that corresponded to the shortest straight-line distance between it and Mornington, calculated using Google Earth. In certain cases, this path would cross into unsuitable habitat where red-backed fairy-wrens do not occur. In these instances, we created a "pivot point" on the interior edge of the species range, and calculated the distance as the sum of the two straight-line distances passing through this point (described in Greig and Webster 2013; Baldassarre et al. 2013). This resulted in a 3052 km transect spanning very nearly the entire species range.

PLUMAGE COLOR QUANTIFICATION

We quantified plumage color following the methods of Baldassarre et al. (2013). From each male's feather sample, we mounted six feathers in an overlapping pattern on a square of black construction paper (Strathmore Artagain® Coal Black). We used an Ocean Optics (Dunedin, FL) USB2000 UV-VIS spectrometer with an R200–7 UV-VIS probe and a PX2 pulsed xenon light source to measure the reflectance of the feather sample. The probe tip was adjusted to illuminate a measurement area of 3 mm^2, and was mounted in a metal block to exclude ambient light. We measured three separate reflectance curves along the avian visible spectrum (300–700 nm) for each feather sample, and averaged the three curves for further analyses.

To account for the unique tuning of the avian visual system, we analyzed reflectance curves using the program TetraColorSpace (Stoddard and Prum 2008), which uses the spectral sensitivity of each of the four cone types in the avian retina to plot each color as a point in a tetrahedral color space. The

Table 1. The sampling transect across the red-backed fairy-wren species range.

No.	Name	Latitude	Longitude	Distance (km)	Ancestry	HI	HI_{diag}	Plumage hue	Genetic *N*	Plumage *N*
1	Mornington	17.3°S	126.6°E	0	*cruent*	0.999 ± 0.001	0.999 ± 0.001	0.926 ± 0.054	15	10
2	Darwin	13.8°S	131.4°E	720	*cruent*	N/A	N/A	0.906 ± 0.069	0	15
3	Camooweal	19.6°S	138.6°E	1293	*cruent*	0.999 ± 0.004	0.997 ± 0.005	0.798 ± 0.121	15	8
4	Mt. Isa	20.4°S	139.3°E	1450	*cruent*	0.991 ± 0.024	0.992 ± 0.027	0.774 ± 0.089	15	7
5	Croydon	18.1°S	142.1°E	1710	Admixed	0.635 ± 0.037	0.571 ± 0.092	N/A	9	0
6	Georgetown	18.2°S	143.1°E	1810	Admixed	0.325 ± 0.082	0.224 ± 0.107	0.735 ± 0.078	15	6
7	Mt. Surprise	18.8°S	144.2°E	1930	*melano*	0.043 ± 0.064	0.028 ± 0.065	0.725 ± 0.067	15	6
8	Donkey Farm	17.3°S	145.2°E	2045	*melano*	0.016 ± 0.018	0.011 ± 0.013	0.655 ± 0.091	10	27
9	Moomin	17.2°S	145.3°E	2051	*melano*	N/A	N/A	0.649 ± 0.124	0	25
10	Ravenshoe	17.4°S	145.3°E	2053	*melano*	N/A	N/A	0.598 ± 0.123	0	10
11	Cardwell	18.2°S	146.3°E	2114	*melano*	0	0.001 ± 0.001	0.505 ± 0.148	14	11
12	Paluma	18.6°S	146.2°E	2139	*melano*	0	0.001 ± 0.001	0.424 ± 0.101	15	8
13	Cromarty	19.3°S	147.3°E	2220	*melano*	0.001 ± 0.001	0.002 ± 0.002	0.307 ± 0.11	11	8
14	Eungella	21.1°S	148.3°E	2386	*melano*	0.001 ± 0.001	0.001 ± 0.001	0.236 ± 0.142	13	7
15	Taunton	23.3°S	149.2°E	2527	*melano*	0.001 ± 0.002	0.002 ± 0.002	0.146 ± 0.095	10	7
16	Brisbane	27.2°S	152.5°E	3052	*melano*	0.001 ± 0.001	0.001 ± 0.001	0.087 ± 0.058	12	23
								Total	169	178

Variation in hybrid index and plumage hue scores is presented as standard deviations. Certain sampling locations were omitted from one of the datasets if they were sampled by a collaborator after genomic analyses began (location 2), no nuptially plumaged males were captured (location 5), or they were located particularly close to another location included in the dataset (locations 9 and 10).

red-backed fairy-wren has a violet-sensitive visual system (Odeen et al. 2012), so we analyzed curves using the average avian violet-sensitive spectral sensitivity curve (Endler and Mielke 2005) assuming idealized illumination (i.e., we did not consider variation in ambient light). TetraColorSpace produces several values that quantify the hue, saturation, and brightness of a color. For this study, we focused on one measure of hue, theta (θ), because previous analyses have shown that it best captures the variation in red to orange that characterizes the subspecies (Baldassarre et al. 2013; Baldassarre and Webster 2013).

GENOTYPING-BY-SEQUENCING

DNA was extracted from blood samples using the Omega Bio-Tek EZ 96 Total DNA/RNA Isolation Kit®, eluted in water, and then concentrated using a vacuum centrifuge. GBS libraries were prepared and analyzed at the Institute for Genomic Diversity (IGD) at Cornell University (Elshire et al. 2011), using the enzyme PstI for digestion. GBS libraries were sequenced at the Cornell University Life Sciences Core Center on two lanes of an Illumina HiSeq 2000 with 96 unique barcodes per lane, resulting in 100 base pair (bp) single-end reads. The resulting raw Illumina data files were filtered into individual SNP genotypes using the nonreference genome Universal Network Enabled Analysis Kit (UNEAK) pipeline (Lu et al. 2013) implemented in TASSEL 3.0 (Bradbury et al. 2007). UNEAK trims all reads to 64 bp after the barcode sequence, clusters identical reads into tags, and then retains the counts of tags for each barcoded individual. The pipeline then performs a pairwise alignment of all tags, and tag pairs with 1 bp mismatches are considered candidate SNPs. Although we did not explicitly consider the effects of discarding tag pairs with multiple mutations, we suspect that such instances were rare due to the short overall length of the reads. Reciprocal pairs of tags were considered true SNPs according to standard protocols at the IGD, with an error tolerance rate of 0.03. After identifying true SNPs, UNEAK returns the count of alleles for each locus in each individual.

Following UNEAK filtering, individual genotypes were recalled using the methods described in Lynch (2009) and White et al. (2013). Genotype likelihood was calculated using a binomial distribution, and a given genotype was called if its Akaike information criterion (AIC) value was at least four lower than the next best genotype, otherwise it was considered missing. We filtered out potential paralogs by discarding loci with a mean heterozygosity >0.75. Although this cutoff is somewhat arbitrary, varying the mean heterozygosity threshold between 0.5 and 1 had no major effect on the results (data not shown). Lastly, we generated two datasets in which either 20 or 40% of the individuals did not have sequence data at a known SNP locus (i.e., missing data).

We sequenced 190 individuals on two lanes of the Illumina HiSeq platform, generating 833,545,374 reads. One hundred and sixty-nine individuals passed initial filtering and were run through the UNEAK pipeline, resulting in 11,136 biallelic SNP loci.

Finally, excluding loci with 20 or 40% missing data resulted in 645 loci with a mean coverage of 19× and 2702 loci with a mean coverage of 12×, respectively. Results for datasets with different amounts of missing data were similar (data not shown), so we present here only the results for the larger dataset that allowed 40% missing data.

POPULATION STRUCTURE ANALYSES

To explore the genetic structure of the hybrid zone and develop a genomic hybrid index, we analyzed all 2702 SNP loci and a subset of 102 "diagnostic" loci. The latter are loci with allele frequency > 0.8 on one end of the cline and <0.2 on the other end (Table S1). We used a Bayesian clustering method implemented in the program STRUCTURE version 2.3.4 (Pritchard et al. 2000; Falush et al. 2003), which assigns individuals to genetic groups minimizing Hardy–Weinberg disequilibrium without using a priori information about sampling locations. Because previous phylogeographic analyses suggested the presence of two separate lineages (Lee and Edwards 2008), and because we were primarily interested in investigating the dynamics of the hybrid zone, we set the number of genetic clusters (K) = 2. However, increasing K did not provide a better explanation of the data as measured by log likelihood (data not shown). We ran 10 iterations with $K = 2$, using the admixture model with correlated allele frequencies, a burn-in period of 100,000, and 100,000 Markov chain Monte Carlo replicates, after which all parameters converged. We used the probability that an individual was assigned by STRUCTURE to the western *cruentatus* cluster (Q) as the hybrid index (Singhal and Moritz 2013). We generated two hybrid indices: one using the inclusive 2702 loci dataset (hereafter HI), and one using the 102 diagnostic locus dataset (hereafter HI_{diag}). We then used an individual's hybrid index score to assign it to a hybrid category (i.e., pure parental or mixed ancestry) following the classification scheme of Aboim et al. (2010) and Taylor et al. (2012). An individual was classified as pure *cruentatus* if $Q \geq 0.9$, pure *melanocephalus* if $Q \leq 0.1$, and mixed ancestry if $0.9 > Q > 0.1$.

GEOGRAPHIC CLINE ANALYSES

Allele frequencies for each SNP locus, the two hybrid indices (HI and HI_{diag}), and plumage hue were fit to a series of equilibrium geographic cline models (Szymura and Barton 1986; Gay et al. 2008) using the Metropolis–Hastings Markov chain Monte Carlo algorithm employed in the R package *HZAR* (Derryberry et al. 2013). We ran 15 separate models that varied in the number of cline shape parameters estimated. All models estimated cline center (distance from sampling location 1, c) and width (1/maximum slope, w), but could additionally estimate different combinations of the exponential decay curve (tail) parameters δ and τ (neither tail, right tail only, left tail only, mirrored tails, or both tails separately). Parameters δ and τ are analogous to d and t described by Gay et al. (2008), and represent the distance from the cline center to the tail and the tail slope, respectively. In addition, the genetic models varied as to whether they did or did not estimate allele frequencies at the cline ends (p_{min} and p_{max}) or fixed them at 0 and 1. The plumage hue models varied as to whether they did or did not estimate mean and variance at the cline ends. These 15 models were then compared using AIC corrected for small sample size (AICc). For each trait, the model with the lowest AICc score was selected as the best-fitting model.

Sample sizes for the genetic clines were corrected following Raufaste et al. (2005) as

$$N_e = \frac{2N}{2N \times F_{ST} + F_{IS} + 1},$$

where N is the number of individuals sampled in a deme, F_{IS} is the deficit of heterozygotes (zero if not positive), and F_{ST} is the fluctuation of allele frequencies between loci, after accounting for differences in their cline shapes. F_{ST} is calculated from the residual variation around the regression line fit during the concordance analysis (see below). For the hybrid indices, we averaged N_e across all loci at each sampling location.

To determine if an individual SNP cline exhibited a different cline shape from the hybrid index, we analyzed the relationship between the hybrid index and allele frequency at each individual locus using the logit-logistic model of Fitzpatrick (2013). Again, we restricted this analysis to SNP loci with frequency >0.8 on one end of the cline and <0.2 on the other end. The predicted allele frequency p in deme i is given by

$$p_i = \frac{S^{v_i}}{S^{v_i} + (1 - S)^{v_i} e^{u_i}},$$

where S is the mean hybrid index over all loci, u gives the relative difference in cline position, and v gives the relative difference in slope. Perfect concordance between a focal locus and the mean hybrid index would result in $u = 0$ and $v = 1$. Parameters u and v were fit using the function "mle2" in the R package *bblme*. Two further models were also fit where either u or v was constrained to be 0 or 1, respectively, and these were compared to the unconstrained model using likelihood ratio tests. P values were adjusted using the Bonferroni correction.

We used two approaches to test for coincidence between the center of the plumage cline and the genetic clines. First, we compared the two log-likelihood unit support limits (hereafter CIs) for the plumage cline center to the CIs for the hybrid index and average SNP cline centers, and considered them noncoincident if they did not overlap. We also compared the CIs for the plumage cline center and each individual SNP locus. Second, we re-fit the best-fitting plumage cline model using *HZAR*, but fixed the value for c at the estimated cline center for the two hybrid index clines. We compared the AICc score of each constrained model with the free model and considered it a worse fit, and thus evidence of

noncoincidental clines, if it had an AICc score more than two points higher.

LINKAGE DISEQUILIBRIUM, DISPERSAL, AND SELECTION IN THE HYBRID ZONE

To calculate the width of a neutral cline and effective selection on a locus, we first estimated dispersal distance in two ways: directly, using four years of mark-recapture data at our field site near Brisbane, Queensland (sampling location 16; Fig. 1); and indirectly, using linkage disequilibrium calculated from our genomic data. Dispersal in this species is sex-biased toward females (Varian-Ramos and Webster 2012), so we included data from 16 observed female natal dispersal events, and calculated direct dispersal distance as the average distance between parent and offspring breeding territories. Linkage disequilibrium ($\bar{D}$) was estimated for each sample site from the variance in the hybrid index (based on the 102 diagnostic loci) using the method of Barton and Gale (1993). $\bar{D}$ at the center of the hybrid zone was estimated by regressing $\bar{D}$ onto average allele frequencies ($\overline{pq}$) over the 102 loci at each site, and then setting $\overline{pq} = 0.25$ (both allele frequencies = 0.5 at the theoretical zone center). Dispersal distance (σ) was then estimated as

$$\sigma = \sqrt{r\bar{D}w^2},$$

where w is the HI_{diag} cline width and r is the recombination rate, set to 0.5 for unlinked loci (Szymura and Barton 1986).

Determining the width of a neutral cline also requires estimating the number of generations since secondary contact. Assuming that widespread aridity across the Carpentarian Barrier was the primary barrier separating the subspecies during the Pleistocene, we estimated that the most recent time for secondary contact was 21 kya, when aridity was most severe, and after which time the climate ameliorated rapidly (Bowler 1976; Torgersen et al. 1988; Chivas et al. 2001; Williams et al. 2009). For the red-backed fairywren, this corresponds to the number of generations, as generation time is one year (D. Baldassarre, pers. obs.). We then combined the above estimates of dispersal and time since secondary contact to calculate the width of a cline resulting from neutral diffusion, where free introgression of alleles across the hybrid zone results in wide, symmetrical clines (Endler 1977; Barton and Gale 1993). In this case, the width of a cline (w) can be modeled as a result of number of generations since secondary contact (t) and dispersal distance (σ) following Barton and Gale (1993):

$$w = 2.51\sigma\sqrt{t}.$$

This cline width can then be compared to the observed cline width to determine the likelihood that the observed cline is the result of neutral diffusion or, if narrower, the result of a barrier to gene flow. We considered an observed cline width to be narrower than the neutral cline if its upper 95% confidence limit did not overlap with the above-calculated cline width. Finally, we used our estimate of dispersal distance to calculate the effective selection pressure on a locus following Barton (1979b), relating cline width (w) to dispersal distance (σ) and selection (s):

$$w = \sigma\sqrt{(8/s)}.$$

Results

GENOMIC ANALYSIS OF HYBRID ZONE

STRUCTURE analyses showed a clear geographic pattern of hybridization that did not differ qualitatively depending on whether all 2702 or the subset of 102 diagnostic SNP loci were analyzed (Fig. 2, Tables 1, S2). The 2702 loci analysis revealed that all individuals from sampling locations 1–4 had a high (≥0.9, mean = 0.99 ± SD 0.01) probability of belonging to the *cruentatus* genetic cluster (i.e., hybrid index, Q), whereas 98% of individuals from sampling locations 7–16 had a low probability (Q value ≤ 0.1, mean = 0.01 ± SD 0.023). All individuals from locations 5 and 6 had mixed ancestry, with mean Q values of 0.64 ± SD 0.04 and 0.33 ± SD 0.08, respectively.

Individual SNP clines were highly variable in both center (mean = 1721.7 ± SD 305.3 km, range = 736.3–2989.8 km) and width (mean = 578.9 ± SD 110 km, range = 12.3–3249.9 km; Figs. 3, S1, Table S3). There was considerable variation in the identity of the best-fitting model for each locus, but the most common model, chosen for 62/102 loci, fixed p_{min}/p_{max} at 0 and 1 and estimated no tail parameters. This was also the best-fitting model for both the HI and HI_{diag} clines (Table 2). Estimates for center and width of the two hybrid index clines were very similar, with overlapping CIs: HI c = 1753.2 (1673.9–1813) km, w = 251.3 (131.7–451.6) km; HI_{diag} c = 1730.4 (1648.5–1790.7) km, w = 238.5 (114.4–438.8) km. Corroborating the STRUCTURE results, the average SNP, HI, and HI_{diag} cline centers were all located between sampling locations 5 and 6 (Fig. 3). Likelihood ratio tests based on the logit-logistic model indicated that 42% (43/102) of SNP clines could not be constrained to have the HI cline center: 28 were shifted significantly west and 15 were shifted significantly east (Table S3). Similarly, 57% (58/102) could not be constrained to have the hybrid index cline width: 42 were significantly wider and 16 were significantly narrower (Table S3).

LINKAGE DISEQUILIBRIUM, DISPERSAL, AND SELECTION IN THE HYBRID ZONE

Our mark-recapture estimate of dispersal distance was 0.75 km. Linkage disequilibrium ($\bar{D}$) was greatest in the hybrid zone center and declined toward the edges (Fig. 4A). There was a significant positive relationship between $\bar{D}$ and average allele frequencies ($\overline{pq}$, regression line: $y = 0.02x - 0.001$, $r^2 = 0.4$, $p = 0.01$;

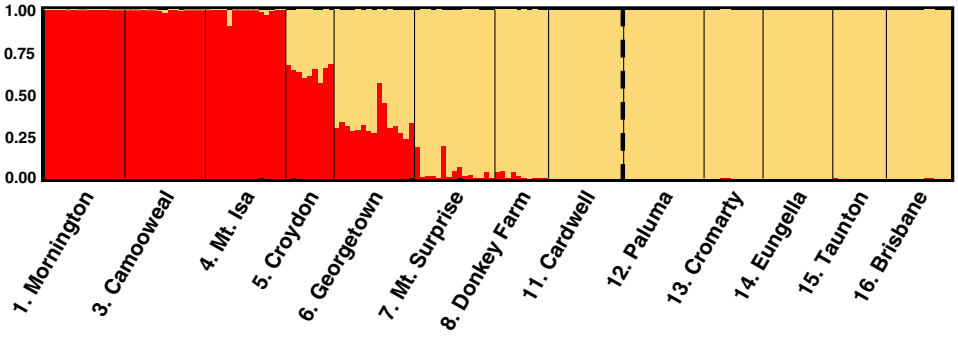

Figure 2. Results of a Bayesian analysis of assignment probability (on the *y*-axis) to either the western *cruentatus* genetic cluster (red) or the eastern *melanocephalus* genetic cluster (orange), using the program STRUCTURE with the 2702 loci dataset. Results are not shown for the 102 diagnostic loci dataset because they were qualitatively similar. Each colored vertical bar represents an individual, with black bars separating sampling locations. The dashed vertical line represents the approximate location of the plumage contact zone.

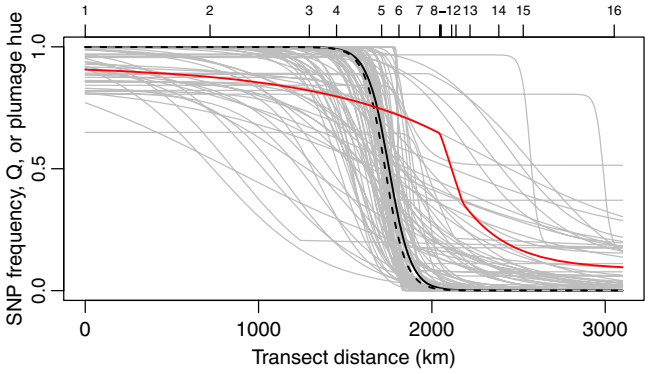

Figure 3. Combined maximum likelihood geographic clines for the 2702 loci hybrid index (HI, black), the 102 diagnostic loci hybrid index (HI_{diag}, black dashed), each of the 102 diagnostic SNP loci (gray), and plumage hue (red). Higher values for hue correspond to redder plumage color. All SNP loci have allele frequency >0.8 on one end of the cline and <0.2 on the other end, even those with very wide-fitted clines that appear to deviate from this criterion. Numbers along the top refer to sampling locations.

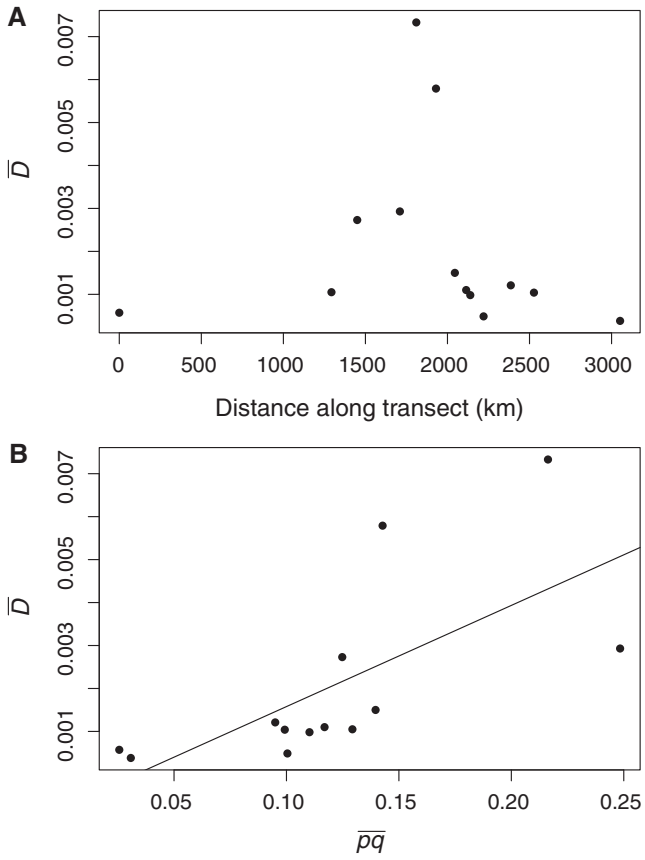

Figure 4. Average linkage disequilibrium across the 102 diagnostic loci plotted against transect distance (A) and average allele frequencies (B).

Fig. 4B). The $\bar{D}$ value in the zone center, where $\overline{pq} = 0.25$, was 0.005 (0.0007–0.0095). Calculating dispersal distance based on this estimate, and taking CIs for both $\bar{D}$ and the HI_{diag} cline width into account, yielded an estimate of 12.04 (2.14–30.24) km. Because of the large discrepancy between the two dispersal estimates, we calculated the width of a neutral cline and effective selection pressure separately for each measure of dispersal. Using the direct estimate of dispersal yielded a neutral cline width of 272.8 km. Both hybrid index clines and 95/102 SNP clines had widths with CIs that encompassed this value. However, seven SNP clines were significantly narrower than the cline predicted by neutral diffusion. Effective selection on the hybrid index was 0.007 (0.002–0.03)%. Across individual SNP loci there was substantial variation in effective selection (mean = 0.08 ± SD 0.35%, range = 4×10^{-5}–3%). Using the $\bar{D}$-based indirect estimate of dispersal yielded a neutral cline width of 4380.3 (778.4–10,999.5) km. Both hybrid index clines and 60/102 SNP clines were significantly narrower than this estimate of neutral cline width. Based on the indirect dispersal estimate, effective selection on the hybrid index was 1.8 (0.06–11.6)%. Because the indirect estimate of dispersal had a very wide confidence interval, effective

Table 2. Parameter estimates for the best-fitting hybrid index and plumage hue clines using *HZAR*.

Trait	Best model	c (km)	w (km)	p_{min}	p_{max}	δ_L	τ_L	δ_R	τ_R
HI	p_{min}/p_{max} observed, no tails	1753.2 (1673.9–1813.2)	251.3 (131.7–451.6)	0.0 (fixed)	1.0 (fixed)	None	None	None	None
HI_{diag}	p_{min}/p_{max} observed, no tails	1730.4 (1648.5–1790.7)	238.5 (114.4–438.8)	0.0 (fixed)	1.0 (fixed)	None	None	None	None
Plumage hue	Mean/variance observed, separate tails	2110.5 (2095.5–2129.1)	376.2 (286.6–511.2)	N/A	N/A	64.4 (39.9–124.8)	0.1 (0.0–0.2)	69.1 (3.7–171.4)	0.4 (0.3–0.6)

Two log-likelihood unit support limits are presented in parentheses. Cline width (w) is 1/maximum slope, cline center (c) is measured in distance (km) from sampling location 1, p_{min} and p_{max} are the allele frequencies at the ends of the cline, and δ and τ are the shape parameters for the left and right tails.

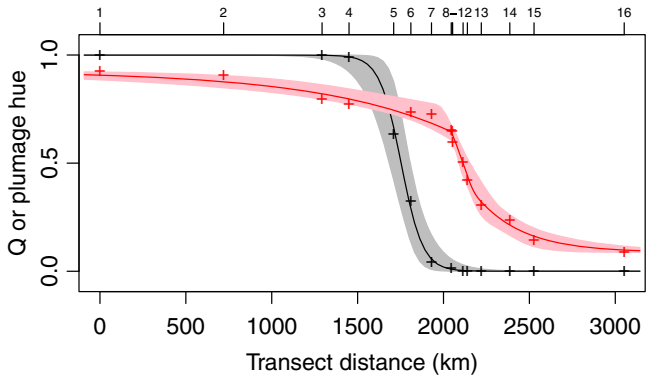

Figure 5. The maximum likelihood cline and the 95% credible cline region for the 2702 loci hybrid index (HI, black) and plumage hue (red). Higher values for hue correspond to redder plumage color. Numbers along the top refer to sampling locations.

selection on individual SNP loci varied dramatically, resulting in some unrealistically high selection estimates for the narrowest clines (results not shown). However, using the lower bound indirect dispersal estimate of 2.14 km resulted in a mean of 0.6% (SD = 2.8, range = 3×10^{-4}–24.4%).

COMPARING GENETIC AND PLUMAGE CLINES

For plumage hue, the best-fitting model did not estimate mean or variance at the cline ends and modeled both sets of tail parameters separately (Table 2). This cline had a center of 2110.5 (2095.5–2129.1) km, which was 357.3 km east of the HI center, 388.8 km east of the average SNP cline center, and located 4 km west of sampling location 11 (Figs. 3, 5). The width of the plumage cline was 376.2 (286.6–511.2) km. The CI for the plumage cline center did not overlap with CIs for the HI, HI_{diag}, or average SNP cline centers (Table 2). Comparing CIs between the center of the plumage cline and individual SNP loci clines revealed that the plumage cline was shifted significantly east relative to 88% (90/102) of the SNP clines. Seven SNP clines had centers coincident with the plumage cline, and five had centers shifted significantly east of the plumage cline. No SNP cline had the same overall shape as the plumage cline, as the seven SNP clines with centers coincident with the plumage cline were much wider than the plumage cline (Fig. 3). Constraining the center of the plumage cline to have either the HI or HI_{diag} cline center produced a significantly worse fit (ΔAICc = 56.5 and 71.3, respectively; Table 3).

Discussion

CHARACTERISTICS OF THE HYBRID ZONE

The hybrid zone as determined by genetic markers is centered at the Carpentarian Barrier, and is likely a result of secondary contact following allopatric genetic and morphological divergence,

Table 3. AICc scores for the best-fitting unconstrained plumage hue cline, and the plumage hue cline constrained to have either the HI or HI_{diag} cline center.

Model	*c* (km)	AICc
Unconstrained	2110.5	−309.1
HI constrained	1753.2	−252.6
HI_{diag} constrained	1730.4	−237.8

as suggested by Lee and Edwards (2008). Overall, 58 and 43% of the SNPs had the same cline center and width, respectively, as the hybrid index cline, indicating that there is considerable genome-wide coincidence and concordance at the Carpentarian Barrier. Both hybrid indices and 61% of the SNP clines best fit a symmetrical model with no tail parameters, indicating negligible introgression outside of the center. These patterns are consistent with a tension zone where multiple unlinked loci form steep coincident clines at the hybrid zone center (Barton 1983; Barton and Hewitt 1985; Barton and Gale 1993). However, the fact that many of the individual SNP clines could not be constrained to have the same center or width suggests that the extent of introgression across the hybrid zone varies among loci. Of the SNP clines that did not have the same center as the hybrid index cline, most were small shifts of less than one cline width to either side. These staggered clines may be due to selection against certain deleterious allele combinations, but especially in cases where the cline center is displaced but there is a long tail of introgression, drift, or variance due to missing data are more likely explanations (Barton 1983, 1993; Polechova and Barton 2011). This genomic dataset contains SNPs that appear to exhibit both of these patterns, as cline shape and thus the extent of introgression outside of the zone center, was highly variable among loci. According to the tension zone model, selection against hybrids likely explains the pattern seen in the 16 SNPs that had significantly narrower cline widths than the hybrid index. These loci may be tightly linked to genes located in genomic regions that contribute to reproductive isolation or local adaptation (Harrison 1990; Wu 2001; Payseur 2010). In contrast, introgression at the 58 SNP loci with significantly wider cline widths appears to be relatively unrestricted, likely because they are not tightly linked to loci under selection. Because the SNP loci in this analysis had substantial allele frequency differences ($\geq$0.6) between allopatric *cruentatus* and *melanocephalus* populations, these wide clines are evidence of extensive introgression rather than incomplete lineage sorting. Thus, the variation in cline width observed in this system is a clear example of a semipermeable genomic boundary between divergent taxa.

HYBRID ZONE MAINTENANCE

We found substantial variation in our estimates of dispersal distance, with the indirect estimate being 16 times higher than the direct estimate. It is important to note that any inferences about neutral diffusion and selection in the hybrid zone depend heavily on an accurate measure of dispersal. Our direct measure of 0.75 km is likely an underestimate due to the limited size of the study area and our inability to detect long distance migrants or account for historic colonization events that would result in higher effective dispersal (Barton and Gale 1993). Nonetheless, even with this conservative estimate of dispersal, seven SNP clines were significantly narrower than the neutral cline, suggesting that selection in these areas of the genome is strong enough to restrict introgression. With an alternative estimate of dispersal based on linkage disequilibrium, both hybrid index clines and 59% of the SNP clines were narrower than would be predicted by neutral diffusion. These patterns are, again, consistent with the tension zone model, where selection against hybrids in the center of the zone prevents free introgression. Nonetheless, selection against hybrids appears to be weak in this system, as almost half of the SNP clines were similar to or wider than the neutral cline (based on the indirect dispersal estimate), indicating that introgression is relatively unrestricted in certain parts of the genome.

Analysis of effective selection in the hybrid zone also suggests that overall selection is low and variable across loci. Our direct dispersal-based estimate of average effective selection of 0.08% (range = 4×10^{-5}–3%) is lower than most published studies of other hybrid zones (e.g., *Heliconius* butterflies = 20–30%, Mallet et al. 1990; *Bombina* toads = 17–22%, Szymura and Barton 1991; *Carlia* skinks = 22–70%, Phillips et al. 2004; *Mus* house mice = 6–9%, Macholán et al. 2007; *Vandiemenella* grasshoppers = 6–41%, Kawakami et al. 2009). Recalculating effective selection using the indirect measure of dispersal increases the estimates, but they are still lower on average than those reported in these other systems. Although it may be true that average selection in the hybrid zone between subspecies of the red-backed fairy-wren is lower than between these more highly diverged taxa, we do not place too great an emphasis on the quantitative values because they are so heavily dependent on an accurate measure of dispersal. Because the direct estimate of dispersal is a conservative one, estimates of effective selection derived from it should be considered a lower limit, whereas estimates of selection derived from indirect measures of dispersal likely represent an upper limit. Furthermore, the total fitness reduction of hybrids is likely to be many times higher than the effective selection pressure on a particular locus. The strongest conclusion we can make based on these analyses is that selection against hybrids is strong enough to maintain several narrow coincident clines despite extensive gene flow in other parts of the genome. Direct field-based measures of hybrid fitness would be necessary to more accurately quantify the strength of selection in the zone center.

In addition to the results from the geographic cline analyses of genetic markers presented here, there are also several other

lines of evidence supporting the tension zone model. Playback experiments have shown that territorial males are significantly more likely to respond to their own subspecies' song, and that variation in song is strongly bimodal and coincident with the genetic hybrid zone (Greig and Webster 2013). These data suggest that song is a social signal functioning as a speciation phenotype (sensu Shaw and Mullen 2011). Additionally, although the Carpentarian Barrier was most prominent as a barrier to dispersal during the Pleistocene, the area is currently sparsely vegetated, frequently flooded, and supports a relatively low density of red-backed fairy-wrens (Chivas et al. 2001; D. Baldassarre, pers. obs.). Tension zones often stabilize in areas of low population density (Barton 1979a; Barton and Hewitt 1985, 1989). Together these observations suggest that the hybrid zone may be located in an area where extrinsic social and ecological selection result in hybrid disadvantage.

ASYMMETRICAL INTROGRESSION OF PLUMAGE COLOR

Our geographic cline analyses are consistent with the hypothesis that alleles for red plumage color have introgressed asymmetrically across the hybrid zone following secondary contact, as the plumage cline was displaced significantly east of the hybrid index clines and the vast majority of the individual SNP clines (Figs. 3, 5). Five SNP clines had centers located east of the plumage cline, supporting the idea that eastward genetic introgression in some parts of the genome could have been substantial enough to recombine "red alleles" from the *cruentatus* subspecies into the genomic background of the orange *melanocephalus* subspecies. Previous work has shown that experimentally reddened males in an allopatric population of the *melanocephalus* subspecies sire significantly more extra-pair offspring than orange males (Baldassarre and Webster 2013). The greater reproductive success of red males may provide the selective force driving the observed introgression, eroding one potential barrier between the subspecies. This hybrid zone appears to be a rare example of the potential for hybridization to introduce adaptive traits into an alternate environment and genomic background due to a sexually selected advantage (but see Stein and Uy 2006). Introgression of a sexual trait from one parental taxon into the other across a hybrid zone can thus eliminate one potential speciation phenotype (Shaw and Mullen 2011), and restrict, rather than promote, the speciation process (Servedio et al. 2013).

There are several alternative explanations for the lack of coincidence between the genetic and plumage clines. First, variation in plumage color may not have a strong genetic basis, but rather be determined predominately by environmental variation due to, for example, dietary intake of carotenoids (Hill 1992). Under this scenario, the plumage contact zone may lie on an ecotone that happens to occur in an area other than the location of secondary contact. We have argued elsewhere that this is unlikely due to the fact that variation in plumage color is not well explained by environmental variation, but rather follows a clear pattern of isolation by distance, consistent with strong genetic underpinnings (Baldassarre et al. 2013). Second, the plumage contact zone may represent the true location of secondary contact, and alleles at the SNP loci analyzed here may have subsequently introgressed westward. Under this scenario, we would expect to find many SNP clines that share the same center as the plumage cline, but our geographic cline and STRUCTURE results refute this idea, corroborating the results from Lee and Edwards (2008) that there is no significant genetic structure across the plumage contact zone. Additionally, the Carpentarian Barrier is older than any biogeographic barrier along the east coast (Cracraft 1986). Given what is known about the time of divergence between subspecies (Lee and Edwards 2008), secondary contact at the Carpentarian Barrier followed by asymmetrical introgression of red plumage color is a more likely explanation.

Finally, plumage color may be selectively neutral, and the displaced cline may be a consequence of genetic dominance of red over orange alleles. This alternative is more difficult to eliminate due to our ignorance of the genetic architecture of plumage color in this species, but has been invoked to explain displaced plumage clines in hybrid zones between species pairs of *Gymnorhina* magpies (Hughes 1982) and *Setophaga* warblers (Rohwer and Wood 1998). Despite our experimental evidence that plumage color is under strong sexual selection on the eastern side of the hybrid zone (Baldassarre and Webster 2013), genetic dominance may still contribute to the displaced cline depending on how many loci are involved. If red plumage were dominant over orange plumage, the frequency of "orange alleles" just west of the center of the plumage cline could be high enough to result in some homozygous recessive individuals with orange plumage. Because plumage hue was measured on a continuous scale, it is difficult to determine the true frequency of "pure orange" birds at this location, but if we consider a bird with a plumage hue value that overlaps with the distribution of hues in the farthest allopatric *melanocephalus* population (sampling location 16), there are no orange birds west of the plumage cline center. However, at sampling location 11, located at the plumage cline center, the frequency of orange birds is $1/11 = 0.09$ (Fig. 6). If we further assume that the frequency of orange alleles in this population is equal to the average *melanocephalus* SNP allele frequency of 0.86, and that each locus has an additive effect on plumage color, then eight unlinked loci would be required to produce the observed phenotype frequencies ($[(0.86)^2]^8 = 0.09$). Although this inference is based on a relatively small sample size, it is substantially higher than the number of genes coding for plumage color in other species (Johnson and Brush 1972; Rohwer and Wood 1998; Domyan et al. 2014). There may also be epigenetic effects that

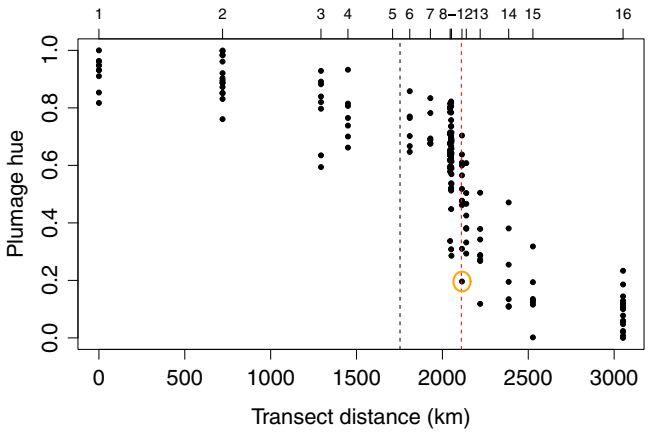

Figure 6. Variation in plumage hue across the transect, with the hybrid index (black) and plumage cline (red) centers marked with dashed lines. Higher values for hue correspond to redder plumage color. At sampling location 11, at the center of the plumage cline, the frequency of orange birds is 1/11 = 0.09 (represented by the circled point). Eight unlinked loci would be required for genetic dominance of red plumage alleles to explain this phenotypic frequency (see text for details). Numbers along the top refer to sampling locations.

affect plumage color that would not be explained by simple underlying allele frequencies. Epigenetic effects on plumage color in birds are very poorly understood, but have been suggested to explain variation in plumage color among albatross species (Family: Diomedeidae; Penhallurick 2012). Without a more detailed study of the genetics of plumage color or crossing experiments, the likelihood of these alternatives is difficult to evaluate. Given the information currently available, we therefore conclude preliminarily that the displaced plumage cline is the result of asymmetrical introgression of alleles for red plumage driven by sexual selection. We acknowledge that contributions from genetic dominance and epigenetic effects are possible, and highlight these areas as priorities for future research in this system.

Traits subject to positive selection on one side of a hybrid zone are expected to quickly sweep to fixation (Barton 1979b; Hewitt 1988), but red plumage color has not yet done so. The red-backed fairy-wren is sedentary and exhibits limited dispersal (Varian-Ramos and Webster 2012), particularly relative to the spatial scale of the transect analyzed here, likely limiting the speed of introgression. The spread of these alleles may be further slowed if they are sex-limited to males, as dispersal is female-biased in this species (Varian-Ramos and Webster 2012). It is also possible that delayed plumage maturation, where male nuptial plumage is often not expressed until at least the second breeding year (Karubian et al. 2008), may slow the spread of the signal. Additionally, farther eastward introgression may be limited by another zoogeographic barrier, the Burdekin Gap (Galbraith 1969; Cracraft 1986), which is a large area of arid habitat located just south of sampling location 13 (Fig. 1) that separates the northern and central Queensland forest biomes, and is known to be a dispersal barrier for several taxa (Chapple et al. 2011). The leading edge of the plumage cline is also located at this area, 2317 km along the transect (Figs. 3, 5). Finally, although field experiments have demonstrated a strong mating advantage for red males in an allopatric orange population (Baldassarre and Webster 2013), the effect of plumage color on fitness in the center of the plumage cline is unknown. If there is relaxed selection on plumage color in the contact zone, this could slow introgression and may also explain the relatively large estimated width of the plumage cline.

Conclusions

In summary, we used a large multilocus SNP dataset combined with reflectance spectrophotometry to analyze genetic and plumage color variation across a hybrid zone between two subspecies of the red-backed fairy-wren. We found coincident and concordant clines for many putatively unlinked SNPs centered at the Carpentarian Barrier, a region previously hypothesized to be the location of secondary contact (Lee and Edwards 2008). Introgression was highly variable among loci, characteristic of a semipermeable boundary between genomes. Although SNP clines varied greatly in width, even with a conservative estimate of dispersal, several clines were narrower than would be predicted by neutral diffusion, suggesting the hybrid zone is a tension zone maintained by a balance of dispersal and weak selection against hybrids. Analysis of the cline for plumage color suggested asymmetrical introgression of red plumage into the genomic background of the orange subspecies, consistent with evidence for strong sexual selection favoring red males east of the hybrid zone (Baldassarre and Webster 2013). The displaced plumage cline may also be affected by genetic dominance of red alleles or epigenetic effects. The red-backed fairy-wren hybrid zone thus exemplifies the potential for sexual selection to erode rather than create a potential reproductive barrier between taxa (Servedio et al. 2013). This study highlights the importance of analyzing hybrid zones between taxa subject to strong sexual selection at an intermediate stage of divergence, as these systems provide unique opportunities to examine the possibility that sexual selection can promote adaptive introgression. Furthermore, incorporating genomic and phenotypic data into analyses will increase our understanding of differential introgression across the genome.

ACKNOWLEDGMENTS

R. Brumfield, R. Harrison, I. Lovette, two anonymous reviewers, and members of the Webster and Lovette laboratories greatly helped improve this manuscript. We thank the many landowners who allowed

us to work on their property, particularly the Australian Wildlife Conservancy, R. Luxton, T. Daniels, Queensland Parks and Wildlife Service, and Seqwater. R. McNeill and the staff at Queensland University of Technology's Samford Ecological Research Facility provided logistical support in the field. Many researchers and field assistants helped collect data, especially W. Lindsay, E. Greig, S. Lantz, J. Wilcox, and A. White. All research activities involving live birds were approved by the Animal Ethics Committee at James Cook University, and IACUC at Cornell University. Research was supported by a National Science Foundation (USA) grant to MSW and JK, as well as grants awarded to DTB from Cornell University, Sigma Xi, and the Cornell Lab of Ornithology Athena Fund. No authors have any conflict of interest to declare.

LITERATURE CITED

Aboim, M. A., J. Mavarez, L. Bernatchez, and M. M. Coelho. 2010. Introgressive hybridization between two Iberian endemic cyprinid fish: a comparison between two independent hybrid zones. J. Evol. Biol. 23:817–828.

Anderson, E., and G. L. Stebbins Jr. 1954. Hybridization as an evolutionary stimulus. Evolution 8:378–388.

Arnold, M. L. 2004. Transfer and origin of adaptations through natural hybridization: were Anderson and Stebbins right? Plant Cell 16:562–570.

Arnold, S. J., P. A. Verrell, and S. G. Tilley. 1996. The evolution of asymmetry in sexual isolation: a model and a test case. Evolution 50:1024–1033.

Baldassarre, D. T., and M. S. Webster. 2013. Experimental evidence that extra-pair mating drives asymmetrical introgression of a sexual trait. Proc. R. Soc. B Biol. Sci. 280:20132175.

Baldassarre, D. T., H. A. Thomassen, J. Karubian, and M. S. Webster. 2013. The role of ecological variation in driving divergence of sexual and non-sexual traits in the red-backed fairy-wren (*Malurus melanocephalus*). BMC Evol. Biol. 13:75.

Barton, N. H. 1979a. The dynamics of hybrid zones. Heredity 43:341–359.

———. 1979b. Gene flow past a cline. Heredity 43:333–339.

———. 1983. Multilocus clines. Evolution 37:1–19.

———. 1993. Why species and subspecies? Curr. Biol. 3:797–799.

———. 2001. The role of hybridization in evolution. Mol. Ecol. 10:551–568.

Barton, N. H., and K. S. Gale. 1993. Genetic analysis of hybrid zones. Pp. 13–45 *in* R. G. Harrison, ed. Hybrid zones and the evolutionary process. Oxford Univ. Press, New York, NY.

Barton, N. H., and G. M. Hewitt. 1985. Analysis of hybrid zones. Annu. Rev. Ecol. Syst. 16:1–37.

———. 1989. Adaptation, speciation, and hybrid zones. Nature 341:497–503.

Bowler, J. M. 1976. Aridity in Australia: age, origins and expression in aeolian landforms and sediments. Earth-Sc. Rev. 12:279–310.

Bowman, D. M. J. S., G. K. Brown, M. F. Braby, J. R. Brown, L. G. Cook, M. D. Crisp, F. Ford, S. Haberle, J. Hughes, Y. Isagi, et al. 2010. Biogeography of the Australian monsoon tropics. J. Biogeogr. 37:201–216.

Bradbury, P. J., Z. Zhang, D. E. Kroon, T. M. Casstevens, Y. Ramdoss, and E. S. Buckler. 2007. TASSEL: software for association mapping of complex traits in diverse samples. Bioinformatics 23:2633–2635.

Brumfield, R. T., R. W. Jernigan, D. B. McDonald, and M. J. Braun. 2001. Evolutionary implications of divergent clines in an avian (*Manacus*: Aves) hybrid zone. Evolution 55:2070–2087.

Chapple, D. G., C. J. Hoskin, S. N. J. Chapple, and M. B. Thompson. 2011. Phylogeographic divergence in the widespread delicate skink (*Lampropholis delicata*) corresponds to dry habitat barriers in eastern Australia. BMC Evol. Biol. 11:191.

Chivas, A. R., A. García, S. van der Kaars, M. J. J. Couapel, S. Holt, J. M. Reeves, D. J. Wheeler, A. D. Switzer, C. V. Murray-Wallace, et al. 2001. Sea-level and environmental changes since the last interglacial in the Gulf of Carpentaria, Australia: an overview. Quat. Int. 83–85:19–46.

Cook, B. D., M. Adams, P. B. Mather, J. M. Hughes. 2012. Statistical phylogeographic tests of competing "Lake Carpentaria hypotheses" in the mouth-brooding freshwater fish, *Glossamia aprion* (Apogonidae). Mar. Freshw. Res. 63:450–456.

Cracraft, J. 1986. Origin and evolution of continental biotas: speciation and historical congruence within the Australian avifauna. Evolution 40:977–996.

Dasmahapatra, K. K., J. R. Walters, A. D. Briscoe, J. W. Davey, A. Whibley, N. J. Nadeau, A. V. Zimin, D. S. T. Hughes, L. C. Ferguson, S. H. Martin, et al. 2012. Butterfly genome reveals promiscuous exchange of mimicry adaptations among species. Nature 487:94–98.

Derryberry, E. P., G. E. Derryberry, J. M. Maley, and R. T. Brumfield. 2013. HZAR: hybrid zone analysis using an R software package. Mol. Ecol. Res. 14:652–663.

Domyan, E. T., M. W. Guernsey, Z. Kronenberg, S. Krishnan, R. E. Boissy, A. I. Vickrey, C. Rodgers, P. Cassidy, S. A. Leachman, J. W. Fondon III, et al. 2014. Epistatic and combinatorial effects of pigmentary gene mutations in the domestic pigeon. Curr. Biol. 24:459–464.

Elshire, R. J., J. C. Glaubitz, Q. Sun, J. A. Poland, K. Kawamoto, E. S. Buckler, and S. E. Mitchell. 2011. A robust, simple genotyping-by-sequencing (GBS) approach for high diversity species. PLoS ONE 6:e19379.

Endler, J. A. 1977. Geographic variation, speciation, and clines. Princeton Univ. Press, Princeton, NJ.

Endler, J. A., and P. W. Mielke. 2005. Comparing entire colour patterns as birds see them. Biol. J. Linn. Soc. 86:405–431.

Falush, D., M. Stephens, and J. K. Pritchard. 2003. Inference of population structure using multilocus genotype data: linked loci and correlated allele frequencies. Genetics 164:1567–1587.

Fitzpatrick, B. M. 2013. Alternative forms for genomic clines. Ecol. Evol. 3:1951–1966.

Fitzpatrick, B. M., J. R. Johnson, D. K. Kump, H. B. Shaffer, J. J. Smith, and S. R. Voss. 2009. Rapid fixation of non-native alleles revealed by genome-wide SNP analysis of hybrid tiger salamanders. BMC Evol. Biol. 9:176.

Galbraith, I. C. J. 1969. The Papuan and little cuckoo-shrikes, *Coracina papuensis* and *robusta*, as races of a single species. Emu 69:9–29.

Garner, S. R., and B. D. Neff. 2013. Alternative male reproductive tactics drive asymmetrical hybridization between sunfishes (*Lepomis* spp.). Biol. Lett. 9:20130658.

Gay, L., P. A. Crochet, D. A. Bell, and T. Lenormand. 2008. Comparing clines on molecular and phenotypic traits in hybrid zones: a window on tension zone models. Evolution 62:2789–2806.

Gompert, Z., M. L. Forister, J. A. Fordyce, C. C. Nice, R. J. Williamson, and C. A. Buerkle. 2010. Bayesian analysis of molecular variance in pyrosequences quantifies population genetic structure across the genome of *Lycaeides* butterflies. Mol. Ecol. 19:2455–2473.

Gompert, Z., T. L. Parchman, and C. A. Buerkle. 2013. Genomics of isolation in hybrids. Philos. Trans. R. Soc. B Biol. Sci. 367:439–450.

Greig, E. I., and M. S. Webster. 2013. Spatial decoupling of song and plumage generates novel phenotypes between 2 avian subspecies. Behav. Ecol. 24:1004–1013.

Harrison, R. G. 1986. Pattern and process in a narrow hybrid zone. Heredity 56:337–349.

———. 1990. Hybrid zones: windows on evolutionary process. Oxford Surv. Evol. Biol. 7:69–128.

Hartman, P. J., D. P. Wetzel, P. H. Crowley, and D. F. Westneat. 2011. The impact of extra-pair mating behavior on hybridization and genetic introgression. Theor. Ecol. 5:219–229.

Hedrick, P. W. 2013. Adaptive introgression in animals: examples and comparison to new mutation and standing variation as sources of adaptive variation. Mol. Ecol. 22:4606–4618.

Hewitt, G. M. 1988. Hybrid zones-natural laboratories for evolutionary studies. Trends Ecol. Evol. 3:158–167.

Hill, G. E. 1992. Proximate basis of variation in carotenoid pigmentation in male house finches. Auk 109:1–12.

Hughes, J. M. 1982. An explanation for the asymmetrical "hybrid" zone between white-backed and black-backed magpies. Emu 82:50–53.

Johnson, N. K., and A. H. Brush. 1972. Analysis of polymorphism in the sooty-capped bush tanager. Syst. Zool. 21:245–262.

Karubian, J. 2002. Costs and benefits of variable breeding plumage in the red-backed fairy-wren. Evolution 56:1673–1682.

Karubian, J., T. S. Sillett, and M. S. Webster. 2008. The effects of delayed plumage maturation on aggression and survival in male red-backed fairy-wrens. Behav. Ecol. 19:508–516.

Kawakami, T., R. K. Butlin, M. Adams, D. J. Paull, and S. J. B. Cooper. 2009. Genetic analysis of a chromosomal hybrid zone in the Australian morabine grasshoppers (*Vandiemenella*, *Viatica* species group). Evolution 63:139–152.

Lande, R. 1981. Models of speciation by sexual selection on polygenic traits. Proc. Natl. Acad. Sci. USA 78:3721–3725.

Larson, E. L., T. A. White, C. L. Ross, and R. G. Harrison. 2014. Gene flow and the maintenance of species boundaries. Mol. Ecol. 23:1668–1678.

Lee, J. Y., and S. V. Edwards. 2008. Divergence across Australia's Carpentarian Barrier: statistical phylogeography of the red-backed fairy wren (*Malurus melanocephalus*). Evolution 62:3117–3134.

Lu, F., A. E. Lipka, J. Glaubitz, R. Elshire, J. H. Cherney, M. D. Casler, E. S. Buckler, and D. E. Costich. 2013. Switchgrass genomic diversity, ploidy, and evolution: novel insights from a network-based SNP discovery protocol. PloS Genet. 9:e1003215.

Lynch, M. 2009. Estimation of allele frequencies from high-coverage genome sequencing projects. Genetics 182:295–301.

Macholán, M., P. Munclinger, M. Šugerková, P. Dufková, B. Bímová, E. Božíková, J. Zima, and J. Pialek. 2007. Genetic analysis of autosomal and X-linked markers across a mouse hybrid zone. Evolution 61:746–771.

Mallet, J., N. Barton, G. Lamas, J. Santisteban, M. Muedas, and H. Eeley. 1990. Estimates of selection and gene flow from measures of cline width and linkage disequilibrium in *Heliconius* hybrid zones. Genetics 124:921–936.

Morjan, C. L., and L. H. Rieseberg. 2004. How species evolve collectively: implications of gene flow and selection for the spread of advantageous alleles. Mol. Ecol. 13:1341–1356.

Nosil, P., S. P. Egan, and D. J. Funk. 2007. Heterogeneous genomic differentiation between walking-stick ecotypes: "isolation by adaptation" and multiple roles for divergent selection. Evolution 62:316–336.

Odeen, A., S. Pruett-Jones, A. C. Driskell, J. K. Armenta, and O. Hastad. 2012. Multiple shifts between violet and ultraviolet vision in a family of passerine birds with associated changes in plumage coloration. Proc. R. Soc. B Biol. Sci. 279:1269–1276.

Panhuis, R. M., R. Butln, M. Zuk, and T. Tregenza. 2001. Sexual selection and speciation. Trends Ecol. Evol. 16:364–371.

Parchman, T. L., Z. Gompert, M. J. Braun, R. T. Brumfield, D. B. McDonald, J. A. C. Uy, G. Zhang, E. D. Jarvis, B. D. Schlinger, and C. A. Buerkle. 2013. The genomic consequences of adaptive divergence and reproductive isolation between two species of manakins. Mol. Ecol. 22:3304–3317.

Pardo-Diaz, C., C. Salazar, S. W. Baxter, C. Merot, W. Figueiredo-Ready, M. Joron, W. O. McMillan, and C. D. Jiggins. 2012. Adaptive introgression across species boundaries in *Heliconius* butterflies. PloS Genet. 8:e1002752.

Parsons, T. J., S. L. Olson, and M. J. Braun. 1993. Unidirectional spread of secondary sexual plumage traits across an avian hybrid zone. Science 260:1643–1646.

Payseur, B. A. 2010. Using differential introgression in hybrid zones to identify genomic regions involved in speciation. Mol. Ecol. Res. 10:806–820.

Penhallurick, J. 2012. The number of albatross (Diomedeidae) species. Open Ornithol. J. 5:32–41.

Phillips, B. L., S. J. E. Baird, and C. Moritz. 2004. When vicars meet: a narrow contact zone between morphologically cryptic phylogeographic lineages of the rainforest skink, *Carlia rubrigularis*. Evolution 58:1536–1548.

Polechova, J., and N. Barton. 2011. Genetic drift widens the expected cline but narrows the expected cline width. Genetics 189:227–235.

Pritchard, J. K., S. Stephens, and P. Donnelly. 2000. Inference of population structure using multilocus genotype data. Genetics 155:945–959.

Raufaste, N., A. Orth, K. Belkhir, D. Senet, C. Smadja, S. J. E. Baird, F. Bonhomme, B. Dod, and P. Boursot. 2005. Inferences of selection and migration in the Danish house mouse hybrid zone. Biol. J. Linn. Soc. 84:593–616.

Ritchie, M. G. 2007. Sexual selection and speciation. Annu. Rev. Ecol. Evol. Syst. 38:79–102.

Rohwer, S., and C. Wood. 1998. Three hybrid zones between hermit and townsend's warblers in Washington and Oregon. Auk 115:284–310.

Rowe, M., and S. Pruett-Jones. 2011. Sperm competition selects for sperm quantity and quality in the Australian Maluridae. PLoS ONE 6:e15720.

———. 2013. Extra-pair paternity, sperm competition and their evolutionary consequences in the Maluridae. Emu 113:218–231.

Rowley, I., and E. M. Russell. 1997. Fairy-wrens and grasswrens: Maluridae. Oxford Univ. Press, Oxford and New York.

Schodde, R. 1982. The fairy-wrens: a monograph of the Maluridae. Lansdowne Editions, Melbourne.

Servedio, M. R., J. Hermisson, and G. S. van Doorn. 2013. Hybridization may rarely promote speciation. J. Evol. Biol. 26:282–285.

Shaw, K. L., and S. P. Mullen. 2011. Genes versus phenotypes in the study of speciation. Genetica 139:649–661.

Singhal, S., and C. Moritz. 2013. Reproductive isolation between phylogeographic lineages scales with divergence. Proc. R. Soc. B Biol. Sci. 280:20132246.

Stein, A. C., and J. A. C. Uy. 2006. Unidirectional introgression of a sexually selected trait across an avian hybrid zone: a role for female choice? Evolution 60:1476–1485.

Stoddard, M. C., and R. O. Prum. 2008. Evolution of avian plumage color in a tetrahedral color space: A phylogenetic analysis of new world buntings. Am. Nat. 171:755–776.

Szymura, J. M., and N. H. Barton. 1986. Genetic analysis of a hybrid zone between the fire-bellied toads, *Bombina bombina* and *B. variegata*, near Cracow in southern Poland. Evolution 40:1141–1159.

———. 1991. The genetic structure of the hybrid zone between the fire-bellied toads *Bombina bombina* and *B. variegata*: comparisons between transects and between loci. Evolution 45:237–261.

Taylor, S. A., D. J. Anderson, C. B. Zavalaga, and V. L. Friesen. 2012. Evidence for strong assortative mating, limited gene flow, and strong differentiation across the blue-footed/Peruvian booby hybrid zone in northern Peru. J. Avian Biol. 43:311–324.

Torgersen, T., J. Luly, P. De Deckker, M. R. Jones, D. E. Searle, A. R. Chivas, and W. J. Ullman. 1988. Late quaternary environments of the Carpentaria Basin, Australia. Palaeogeogr. Palaeoclimatol. Palaeoecol. 67:245–261.

Uyeda, J. C., S. J. Arnold, P. A. Hohenlohe, and L. S. Mead. 2009. Drift promotes speciation by sexual selection. Evolution 63:583–594.

Varian-Ramos, C. W., and M. S. Webster. 2012. Extrapair copulations reduce inbreeding for female red-backed fairy-wrens, *Malurus melanocephalus*. Anim. Behav. 83:857–864.

Varian-Ramos, C. W., W. R. Lindsay, and J. Karubian. 2012. Female red-backed fairy-Wrens (*Malurus melanocephalus*) do not appear to pay a cost for high rates of promiscuity. Auk 129:529–536.

Webster, M. S., C. W. Varian, and J. Karubian. 2008. Plumage color and reproduction in the red-backed fairy-wren: Why be a dull breeder? Behav. Ecol. 19:517–524.

West-Eberhard, M. J. 1983. Sexual selection, social competition, and speciation. Q. Rev. Biol. 58:155–183.

White, T. A., S. E. Perkins, G. Heckel, and J. B. Searle. 2013. Adaptive evolution during an ongoing range expansion: the invasive bank vole (*Myodes glareolus*) in Ireland. Mol. Ecol. 22:2971–2985.

Williams, M., E. Cook, S. van der Kaars, T. Barrows, J. Shulmeister, and P. Kershaw. 2009. Glacial and deglacial climatic patterns in Australia and surrounding regions from 35,000 to 10,000 years ago reconstructed from terrestrial and near-shore proxy data. Quat. Sci. Rev. 28:2398–2419.

Wu, C.-I. 2001. The genic view of the process of speciation. J. Evol. Biol. 14:851–865.

Associate Editor: R. Brumfield

Supporting Information

Additional Supporting Information may be found in the online version of this article at the publisher's website:

Table S1. Allele frequencies and effective sample sizes for the 102 diagnostic SNP loci across the transect.

Table S2. Individual *Q* values and 90% confidence limits from STRUCTURE analyses with both the 2702 loci dataset and the 102 diagnostic loci dataset.

Table S3. Best-fitting maximum likelihood cline model parameters for all individual SNP loci, as well as results of analyses of concordance with the genomic hybrid index cline.

Figure S1. The best-fitting maximum likelihood clines and 95% credible cline regions for each individual SNP locus.